nature chemistry

ARTICLES

https://doi.org/10.1038/s41557-019-0292-z

Building in vitro transcriptional regulatory networks by successively integrating multiple functional circuit modules

Samuel W. Schaffter[1] and Rebecca Schulman[1,2]

The regulation of cellular dynamics and responses to stimuli by genetic regulatory networks suggests how in vitro chemical reaction networks might analogously direct the dynamics of synthetic materials or chemistries. A key step in developing genetic regulatory network analogues capable of this type of sophisticated regulation is the integration of multiple coordinated functions within a single network. Here, we demonstrate how such functional integration can be achieved using in vitro transcriptional genelet circuits that emulate essential features of cellular genetic regulatory networks. By successively incorporating functional genelet modules into a bistable circuit, we construct an integrated regulatory network that dynamically changes its state in response to upstream stimuli and coordinates the timing of downstream signal expression. We use quantitative models to guide module integration and develop strategies to mitigate undesired interactions between network components that arise as the size of the network increases. This approach could enable the construction of in vitro networks capable of multifaceted chemical and material regulation.

Cells are able to use genetic regulatory networks (GRNs) composed of interconnected genes that regulate one another to orchestrate complex behaviours such as differentiation[1,2] and adaptation in response to environmental stimuli[3–5]. These networks sense and process environmental signals to select and direct an appropriate response, such as a gene expression program that produces downstream signals to change the cellular state. Complex cellular GRNs are composed of smaller functional units (termed network or circuit modules) that individually exhibit behaviours such as multistability, oscillations, pulses, adaptation, ordered temporal expression or multi-input information processing[6–8]. The integration of multiple functional modules into larger composite networks allows cells to coordinate different tasks in time and respond to a changing environment by engaging distinct modules in the network. Such integrated GRNs coordinate the synthesis of cellular products to control complex behaviours such as stress response[4,5], environmental adaptation[3] and morphogenesis[1,7].

Many of the key functional modules identified in cellular GRNs have been recapitulated using synthetic chemistries in vitro. For example, in vitro GRN analogues that demonstrate oscillatory behaviour[9–14], bistability[15–20] and adaptation[15,21,22] have been extensively characterized and optimized. Other synthetic chemistries that can emulate some of the dynamic properties of cellular GRNs have also been explored to create reaction networks with similar behaviours[23–27].

Some emerging applications of synthetic in vitro GRN analogues are the autonomous dynamic control and adaptive regulation of downstream chemistries and materials. In this context, in vitro GRN analogues could direct synthetic materials to exhibit some of the sophisticated behaviours of living systems[28–33]. For example, synthetic GRN analogues have been programmed to direct dynamic, spatial or multistage self-assembly processes[34–36], coordinate material state transitions[12,37–39], produce stable chemical or material spatial patterns using coupled reactions and diffusion[35,40] or orchestrate spatiotemporal signalling or developmental patterning processes within systems of initially uniform particles or artificial cell-like compartments[40–42].

In vitro transcriptional circuits[14,17,20,21,39,43] have emerged as a simple yet powerful[44] tool for assembling synthetic networks to direct the dynamics of diverse downstream materials or chemistries. These circuits consist of short synthetic transcriptional templates called genelets. Each genelet contains an incomplete promoter site for T7 RNA polymerase (T7 RNAP), where transcription of an RNA output only occurs when a DNA activator strand is bound to the genelet. Transcribed RNAs can regulate the transcription of a target genelet by controlling the availability of the target genelet's DNA activator through nucleic acid hybridization and strand displacement. Regulatory interactions can therefore be programmed by the straightforward process of designing complementary nucleic acid sequences. In addition to signal production (that is, transcription), RNA signals are also degraded by RNase H. Coupled signal production and degradation together establish a signal turnover process analogous to the signal turnover in cellular GRNs (Fig. 1a). Genelet circuits can thus emulate complex cellular GRN dynamics using short DNA sequence elements and two robust, commercially available and well-characterized enzymes[45] that operate reliably in batch reactions under a range of reaction conditions[46–48]. Furthermore, the outputs of genelet circuits—RNA molecules—have applications in a number of material, chemical and biotechnological settings[49,50], and the amount of output produced can be tuned over a large dynamic range[51], meaning genelet circuits could be readily applied in a variety of existing systems across a range of scales.

Genelet modules containing 2 to 3 'nodes' that regulate one another have been programmed to exhibit oscillatory behaviour[14], bistability[17,20], adaptation[21] and feedback control[43], and some of these modules have been successfully coupled to downstream processes[36,39,42]. However, an individual genelet module cannot coordinate the multifunctional regulation seen in cellular GRNs.

[1]Department of Chemical and Biomolecular Engineering, Johns Hopkins University, Baltimore, MD, USA. [2]Department of Computer Science, Johns Hopkins University, Baltimore, MD, USA. e-mail: sschaff6@jhu.edu; rschulm3@jhu.edu

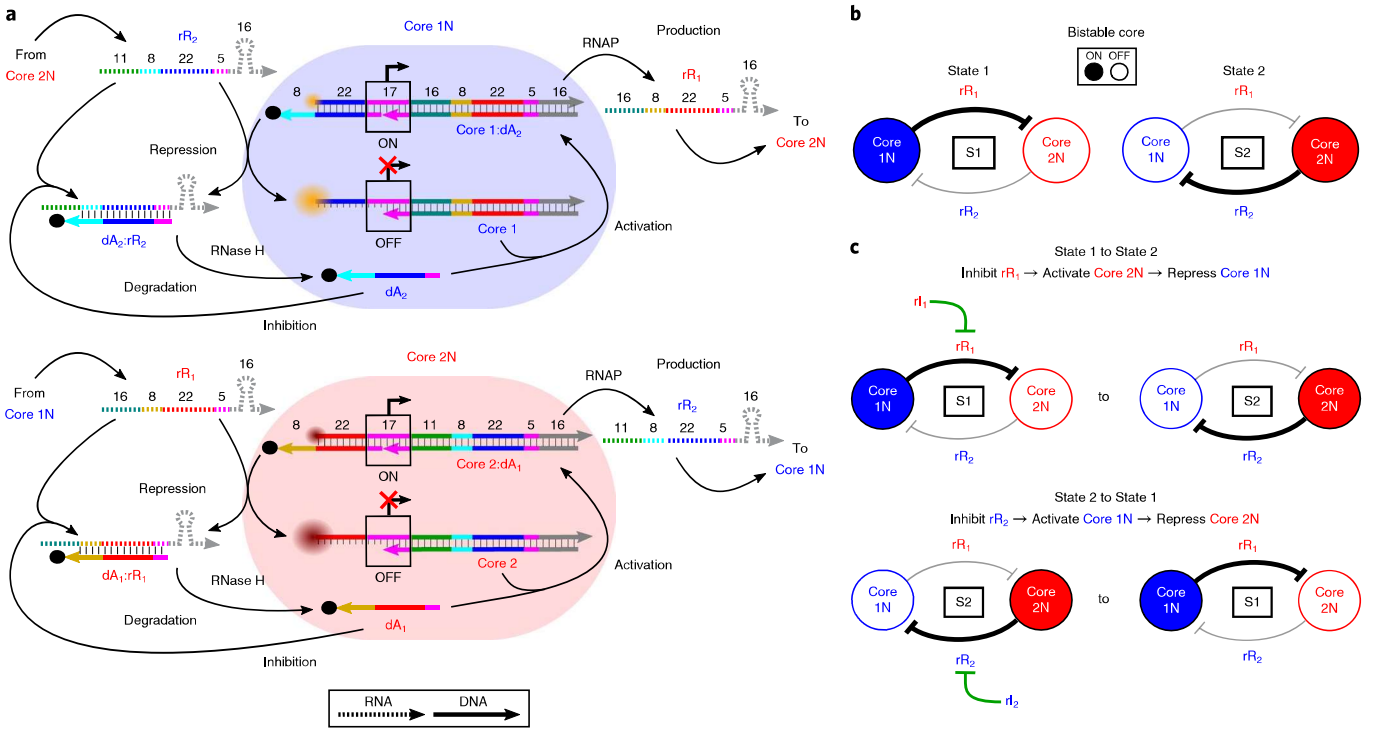

Fig. 1 | Genelets and a switchable bistable network. a, A genelet is a T7 RNAP transcriptional template that is activated (ON) for transcription when a DNA activator (dA_i, where i is 1 or 2) binds and completes the T7 RNAP promoter sequence (pink boxed domain) and inactivated (repressed) when an RNA repressor (rR_i) removes the DNA activator from the genelet–activator complex[20]. RNA bound to DNA is degraded by RNase H, freeing DNA activators. Genelets can be nodes of a network; that is, Core 1N (top) and Core 2N (bottom), when the RNA transcribed from one node represses another. Node activation levels are tracked via fluorescence: fluorophores (red and orange gradient circles on the genelets) and quenchers (black circles on the activators) create high fluorescence when a node is OFF and low fluorescence when a node is ON. Complementary sequence domains are colour coded. The numbers indicate the number of nucleotides in each domain. The prefixes r and d denote RNA or DNA, respectively. **b**, The two stable states (S1 and S2) of the bistable network. Bold regulatory interactions (blunt arrows) indicate high RNA expression. **c**, An inducer RNA (rI_i) can switch the network's state by inhibiting the rR_i expressed in that state.

Considering cellular GRNs build complexity by integrating many functional regulatory modules together[6,7], the ability to incorporate multiple genelet modules together into larger composite networks could make it possible to build sophisticated multifunctional GRN analogues. Such multifunctional networks will be required if the coordinated control of multiple dynamic processes and adaptive responses seen in cellular GRNs is to be achieved in synthetic systems. Yet constructing large multifunctional synthetic networks is challenging, as it requires that individual functional modules can be combined without introducing cross-talk between components, and that interconnected modules can be tuned to successfully communicate with each other to coordinate regulatory tasks.

Here, we demonstrate that multifunctional synthetic genelet regulatory networks can be assembled by successively integrating multiple functional circuit modules into larger networks. We combine new and previously characterized genelet modules to create a composite network that dynamically changes its state in response to different upstream signals and coordinates the temporal regulation of state-specific downstream expression programs. To obtain the desired composite network function, we build and fit quantitative models of network behaviour to guide the development and tuning of individual modules. To reliably integrate multiple modules into our network, we identify sources of undesired interactions between network components and develop design strategies to mitigate these effects. In particular, we develop a new mechanism for genelet regulation that increases the number of orthogonal nodes that can be organized into a network without cross-talk, and allows new functional modules to be integrated into existing systems without hindering the performance of the network. Our approach to network design successfully demonstrates a route to increase the functionality of synthetic GRN analogues through the systematic integration of multiple circuit modules into a composite network. This approach could enable the development of a new class of mesoscale synthetic networks that combine different functional circuit modules to perform increasingly complex chemical and material regulatory processes by design.

Results

A responsive bistable network. Key classes of GRNs identified in many cellular developmental[1,7] and adaptive response[3,4] pathways are those that allow cells to select from or switch between different gene expression programs in response to environmental stimuli. We sought to mimic these capabilities in a synthetic network by developing a genelet regulatory network that could change states in response to upstream signals and direct state-specific downstream signal expression programs. A network with these capabilities requires multiple different integrated functional circuit modules that together coordinate the desired regulatory tasks. A state control module is required to maintain the network's state, induction modules are necessary to induce stimuli-specific state changes, insulation modules are needed to convert network states into downstream signals and downstream signal regulation modules are needed to coordinate the temporal dynamics of downstream signal expression. To begin constructing a network with these properties, we selected

a previously described genelet circuit composed of two mutually repressive nodes as our state control module (Fig. 1b)[20]. This network has been shown to exhibit bistability where—depending on the initial expression levels of the nodes—the network will converge to one of two stable expression states with only one node active, state 1 (S1) or state 2 (S2) in Fig. 1b. The network's state can be set by initially including one of the repressors in excess of its respective activator, and it will remain in the initial state even after the initially added repressor has degraded[20] (Supplementary Fig. 1). We selected this bistable network as the core of our regulatory network, as each stable state could potentially direct a state-specific downstream task.

Although this network is bistable, the ability to repeatedly switch the network between its two states in response to changing upstream signals has not been demonstrated. We therefore sought to develop induction circuit modules that could orchestrate state changes. We focused on developing a means to switch states using RNA molecules that could be produced by upstream genelets that together would constitute our induction modules. These induction modules would then allow the bistable circuit to be further integrated into larger networks. An RNA molecule could switch the network's state by either acting as a repressor of the node that is ON (mechanism 1) or inhibiting the repressor of the node that is OFF (mechanism 2) in a given state (Supplementary Section 3). A key performance metric of a mechanism for switching the state of an in vitro circuit is the time required to complete a state change[16]. Fast switching allows for a rapid response and limits the fuel consumption, enzyme degradation and waste accumulation that occur during operation, all of which eventually degrade the performance of the circuit in batch reactions[9,14,17,39]. We thus compared the switching times for the two switching mechanisms using kinetic simulations of induced state changes. We found that mechanism 2 should induce a state change much more quickly than mechanism 1 (Supplementary Fig. 2). Mechanism 1 is slower because all of the excess repressor produced while the network is in its initial state must be degraded by RNase H before the state change can complete, resulting in a long delay time in switching. By contrast, in mechanism 2, the RNA species that induces a state change acts by inhibiting any excess repressor produced while the network is in its initial state, so the addition of this RNA immediately starts the state change (Supplementary Section 3). In support of the predictions of our simulations, initial experiments evaluating switching via mechanism 1 showed long switching times (Supplementary Fig. 3). To begin developing the induction module, we therefore first sought to design RNA species that could specifically inhibit the repressors of each node and could thus induce network state changes in either direction (Fig. 1c). We termed RNA species with this function inducer RNAs.

Switching network states with inducer RNAs. Functional inducer RNA sequences need to bind and inhibit their repressor targets without interacting with other network components. Considering that repressors and activators are complementary (Fig. 1a), and that inducers must be complementary to repressors (Fig. 2a), inducer RNAs will share sequence elements with the activators in the network. So, although they are designed to bind repressors, the inducer RNAs could prevent or slow down activation by competing with the activators in binding to the genelet's activator binding domains (ABDs). To find inducer RNA sequences that could bind to their target repressors without introducing off-target effects, we designed three different potential inducer RNA sequence variants. Each variant was designed to hybridize to the 8-base toehold binding domain on its respective repressor target (TH in Fig. 2a). The toehold domain initiates the reaction in which the repressor removes its corresponding activator from a genelet-activator complex (Fig. 1a). An inducer RNA binding to the toehold domain should thus prevent the repression reaction from occurring. To ensure stable hybridization at 37 °C, the inducer RNA variants' sequences were extended with full, partial or no complementarity to the ABDs of the repressors (Supplementary Section 1.4).

Inducer RNAs with partial complementarity (rI_1 and rI_2) to the ABDs of the repressors switched the network's state at rates similar to those predicted in our simulations (Supplementary Fig. 4). Variants with either full or no complementarity to the ABDs of their repressors were unable to switch the network's state or switched the state more slowly than our simulations predicted, probably due to off-target interactions (Supplementary Figs. 5 and 6). We therefore selected rI_1 and rI_2 to further characterize switching. We termed this network—consisting of rI_1/rI_2 and the Core nodes—the inducible bistable network (iBN). For reference, a network naming schematic is in Supplementary Section 1.1.

In addition to switching the state of the iBN after 30 min of operation (Supplementary Fig. 4), the inducer RNAs could also switch the network's state after both 2 h and 4 h in its initial state (Fig. 2b,c). At least 3 μM of rI_1 was required to successfully switch the network from S1 to S2 when added 30 min after the network was initialized. Adding less rI_1 did not change the network's state and adding more did not speed up the state change (Supplementary Fig. 7). A higher concentration of rI_1 was required to switch states at times beyond 30 min (Supplementary Fig. 8). State changes could also be induced at room temperature in addition to the optimal transcription temperature of 37 °C (Supplementary Fig. 9).

The state of the network could also be switched twice via sequential addition of the inducer RNAs (Fig. 2d), and the amount of rI_1 added to switch states the first time influenced the timing of the second switch (Supplementary Fig. 10). We were unable to completely switch the state of the network three consecutive times within 10 h of circuit operation (Supplementary Fig. 11). Eventual loss of circuit function is inevitable in batch reactions due to enzyme degradation, fuel exhaustion and/or accumulation of waste products, although oscillating genelet circuits have been shown to function for 15–20 h (refs. [14,39]). As both genelets end up in an ON state at the end of our experiments, the shorter lifetime of the bistable circuit could be due to a decrease in the effective transcription rate over the course of the experiment[52–54] and/or the accumulation of RNA waste products that impede the repression reactions[9,14,39] (Supplementary Section 5.2). Bistable modules may also be particularly sensitive to changes in reaction rates over the course of an experiment, as a synthetic bistable module built using a different set of chemical reactions exhibited much shorter operational lifetimes compared with oscillating modules built using the same types of reactions[16].

Although the inducer RNAs worked as designed, we observed that Core 1N became partially inactivated during experiments where the network was initialized in S1 (Fig. 2b). We found that non-specific transcription of Core 1N components caused this undesired phenomenon (Supplementary Section 6), which we termed Core 1N autoinhibition.

To account for the dependence of inducer RNA dose and timing, Core 1N autoinhibition and other nonlinear effects on iBN dynamics when incorporating it into larger networks, we developed a kinetic model of the iBN (Supplementary Section 7.1). Our model included terms for the designed reactions in the network (Supplementary Fig. 22) and Core 1N autoinhibition reactions (Supplementary Fig. 23). We were able to fit rate parameters that were consistent with those that were determined in previous studies[20,39] (Supplementary Section 7.2), and the model accurately captured the dynamics of the iBN as it switched states in response to different concentrations of inducer provided at different times. The model also recapitulated the observed Core 1N autoinhibition (Fig. 2b–d and Supplementary Figs. 24 and 25).

Integrating the iBN into larger networks. With a successful RNA switching method developed, we next investigated whether upstream genelets (that is, induction modules) could direct the

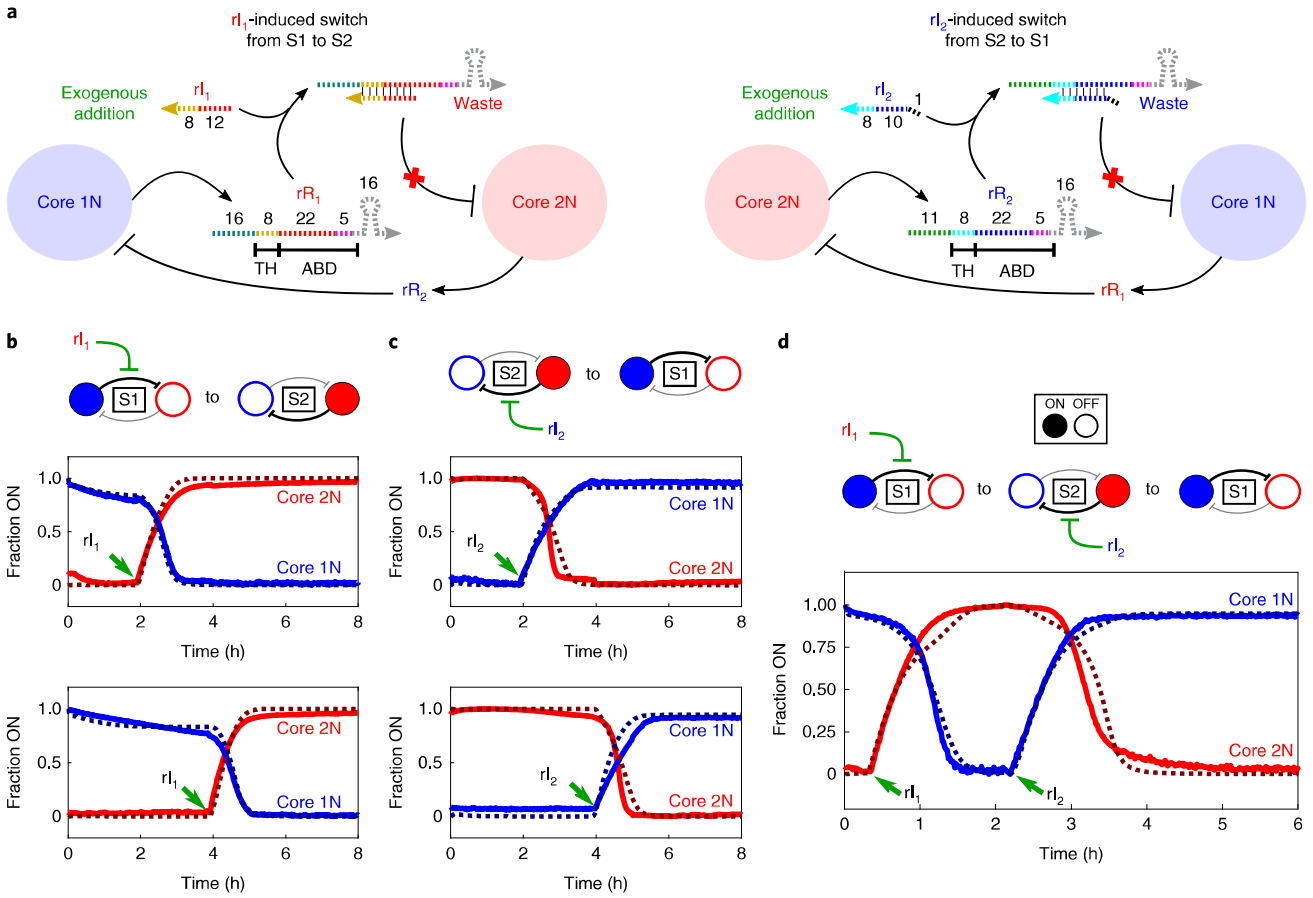

Fig. 2 | Inducer RNAs switch the state of the bistable network. a, Inducer RNAs rI_1 and rI_2 bind to repressors rR_1 and rR_2, respectively. In each case, this binding reaction sequesters the toehold binding domain (TH) of the repressor, preventing it from repressing its intended network node to promote a state change. The inducer RNAs are also partially complementary to the activator binding domains (ABDs) of the repressors. **b**,**c**, Normalized activation levels of network nodes during switches from S1 to S2 via addition of rI_1 (**b**) or from S2 to S1 via addition of rI_2 (**c**). The green arrows indicate times at which rI_1 or rI_2 were added to a final concentration of 5 μM (top plots) or 10 μM (bottom plots). **d**, Normalized activation levels of network nodes during two switches via sequential addition of inducer RNAs (green arrows); rI_1 and rI_2 were added to final concentrations of 3 μM and 10 μM, respectively. The solid lines in the plots are experimental results and the dashed lines are the simulations of our kinetic model (Supplementary Section 7). Additional experimental data with model fits are presented in Supplementary Figs. 24 and 25.

iBN to change states. Connecting the iBN to upstream nodes would also allow the iBN to be integrated into larger networks, enabling further expansion of network functionality[6]. To connect the iBN to upstream nodes, we designed a network architecture in which activatable genelets would transcribe the inducer RNAs required to switch the state of the iBN and verified with simulations that these additional genelets could produce enough inducer to switch states (Supplementary Fig. 26). We termed this expanded network the iBN with upstream activation (iBN-uA) and the new upstream nodes Induce 1N and Induce 2N (Fig. 3a).

We attempted to design the genelet, activator and repressor sequences of the Induce nodes using the nucleic acid modelling software NUPACK 3.2.2[55] (Supplementary Section 8.2). However, NUPACK could only find sequences that were predicted to interact with each other or existing iBN components in undesired ways (Supplementary Section 8.3). Experimental characterization of one set of designed Induce node sequences confirmed this propensity (Supplementary Fig. 27). Cross-talk among the network components was not surprising, considering that the sequences for the iBN were already set and the large number of long single-stranded domains in the network. To assess whether this cross-talk was primarily due to the pre-set iBN sequences, we also tried to design a set of six new orthogonal genelet nodes that exhibited low cross-talk with one another, but we were not able to find suitable sequences (Supplementary Section 8.4). These results suggest that the genelet design was limiting the ability to build larger networks.

We thus sought to develop a design strategy that would make it possible to develop a large number of genelet nodes that had very little cross-talk with one another. One strategy for the design of large nucleic acid reaction networks that do not cross-react is to limit the sequences of single-stranded domains to contain only three of the four bases (typically A, T and C)[56]. However, the genelet architecture makes such an approach difficult to implement, as orthogonal genelet activators and repressors may be single-stranded but each activator/repressor pair must be complementary. The activator and repressor sequences thus cannot both be limited to the same three bases. Consistent with this observation, designing a set of genelet nodes in which all of the repressor sequences comprise only three of the bases did not reduce the number of predicted undesired interactions over designs where the repressor sequences could contain any base (Supplementary Section 8.4).

Another approach to decreasing the potential for cross-talk in nucleic acid circuits is to reduce the lengths of single-stranded domains, such as by creating primarily double-stranded complexes that react via four-way branch migration[57,58]. We used this approach to design Induce genelets with hairpin clamp motifs (HPCs) in

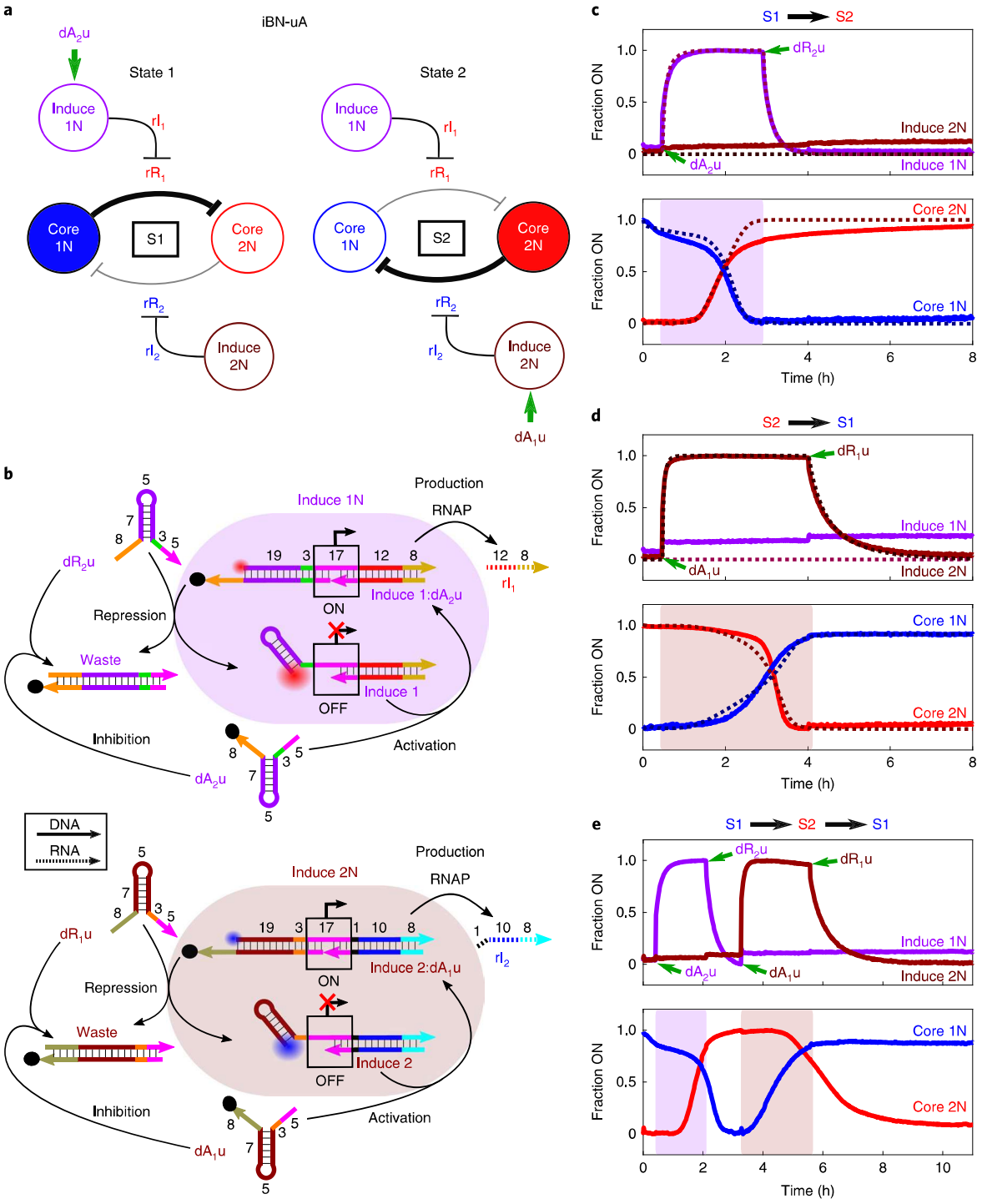

Fig. 3 | Upstream nodes that produce inducer RNAs switch the state of the iBN. a, The architecture of the iBN-uA in each stable state. State changes are induced by activating the respective Induce nodes (indicated by the green arrows). **b**, Induce node reactions with hairpin clamp (HPC) motifs for activation and repression. **c**–**e**, Normalized experimental (solid lines) and simulated (dashed lines) activation levels of network nodes during switches from S1 to S2 via activation of Induce 1N (**c**), from S2 to S1 via activation of Induce 2N (**d**) or from S1 to S2 and back again via sequential activation and repression of Induce 1N, then Induce 2N (**e**). The shaded regions in the bottom plots indicate when the respective Induce node was ON during the experiments. Induce node activators (dA_1u/dA_2u) and repressors (dR_1u/dR_2u) were added at the times indicated by the green arrows in the top plots to final concentrations of 1 μM and 1.5 μM, respectively. To sustain circuit activity over the time required to switch the network's state twice (Supplementary Fig. 33), more RNA polymerase (3.86 U μl^{-1}) was added alongside dA_1u in **e**.

their ABDs (Fig. 3b). The resulting activators have only two 8-base single-stranded domains and the accompanying genelets each have just one 8-base single-stranded domain, as compared to the 27-base single-stranded domains on the Core genelets and their 35-base single-stranded activators. The much shorter single-stranded domains on the HPC genelets and activators reduce their potential to participate in undesired interactions. With the HPC design, NUPACK was able to find sequences for the Induce nodes that were

predicted to have minimal cross-talk with all of the iBN-uA components. These designed HPC genelets exhibited no cross-talk with the other activators in the network in experiments (Supplementary Fig. 28). We also found that the HPC design should increase the number of orthogonal genelet nodes that may be designed with low predicted cross-talk over the number of nodes that can be designed using the original iBN genelet design by at least five or sixfold (Supplementary Section 8.6).

Importantly, despite reacting via four-way branch migration (which could be slower than the three-way branch migration process of the original genelet design), the HPC genelets could also be turned on and off rapidly by their designed activators and repressors (Supplementary Section 8.7). We thus used the Induce nodes with the new HPC motifs in the iBN-uA.

To test the iBN-uA, we selected concentrations for the Induce genelets using simulations based on our model of the iBN (Supplementary Fig. 26). The resulting iBN-uA network was stable in both initial states (Supplementary Fig. 32) and the network's state could be switched in either direction by turning on the appropriate Induce node. Furthermore, the network remained in its new state after the Induce nodes were subsequently turned off (Fig. 3c,d). The network's state could also be switched twice by sequentially turning on and off the respective Induce nodes for each state change (Fig. 3e).

We also investigated whether the rate constants used to model the iBN were consistent with measured iBN-uA dynamics. We extended our kinetic model to include the Induce node reactions (Supplementary Section 9.1) and fit these reactions' kinetic parameters while holding the rate constants determined for the iBN model constant. The resulting model captured the network's dynamics well (Fig. 3c,d), suggesting the model of the iBN is predictive of this network's behaviour in the larger iBN-uA.

Controlling the production of downstream signals. Although the iBN-uA can change states in response to upstream signals, it cannot be coupled to downstream processes without substantially affecting the network's performance. For example, using the iBN-uA's state-dependent signals (rR_1 or rR_2) to control a downstream process would change the concentration of these signals, potentially perturbing the network's state in a phenomenon known as retroactivity[39,59]. Furthermore, using rR_1 or rR_2 to direct downstream processes would require the sequences of the entire iBN to be redesigned for applications that required different downstream RNA signals. To address these issues with downstream coupling, we incorporated insulation modules into our network that have been shown to limit the effects of retroactivity in genelet circuits[39,60]. To integrate the insulation modules into the iBN-uA, we added two downstream nodes—termed Produce nodes—to the network. Produce 1N and Produce 2N have the same activators as Core 1N and Core 2N, respectively, so each Produce node is ON or OFF when its corresponding Core node is ON or OFF (Fig. 4a). In our experiments, the Core nodes' activators are in great excess of the Core genelets (Supplementary Section 1.2), so the Produce genelets can be added to the network without changing the iBN's activator concentrations. As the rate of RNase H-induced degradation is determined by the total activator concentration, incorporation of the Produce nodes will not change the degradation rates of the repressors in the network. Furthermore, the Produce nodes' transcripts are different than the Core nodes', so downstream processes that consume these transcripts will not impose a load on the iBN[39,60] and the network can be programmed to express different RNA signals by simply redesigning the Produce nodes' transcription sequences.

To characterize the rates of the Produce nodes' RNA production, we designed these nodes to express RNA outputs (rO_1 and rO_2 in S1 and S2, respectively) that could be detected with fluorescence reporting (Fig. 4b). We termed this network the iBN-uA with downstream signal production (iBN-uA-dSP). For the iBN-uA-dSP and subsequent networks, we also used a new version of dA_2 with a blocked 3' end that mitigated Core 1N autoinhibition (Supplementary Section 10).

Initialization of the iBN-uA-dSP in either state resulted in the production of only the downstream RNA signal that corresponded to the network's initial state (Supplementary Fig. 36). Switching the state of iBN-uA-dSP similarly switched which downstream RNA signal was being produced (Fig. 4c,d). Notably, the iBN-uA-dSP rapidly creates a high concentration of downstream signal. With just 35 nM of the Produce 1 genelet, a fluorescence signal corresponding to at least 1 μM of rO_1 was reached after 1 h in S1 (Fig. 4c), suggesting this network could drive processes requiring high signal concentrations.

Temporal regulation of downstream signal availability for mutually exclusive signal expression. One limitation to the design of iBN-uA-dSP is that the signal produced in the initial state remains after the network switches to the other state. For example, rO_2, which cannot be degraded by RNase H, persists after the network is switched from S2 to S1 (Fig. 4d), and even rO_1, which is degraded by RNase H when bound to the DNA reporter's fluorescent strand, persists long after the network switched from S1 to S2 (Fig. 4c). The persistence of signals across states prohibits the iBN-uA-dSP from switching between mutually exclusive downstream processes.

To enable mutually exclusive downstream expression states, we incorporated downstream signal regulation modules into the iBN-uA-dSP to rapidly remove downstream signals during state changes. To integrate the downstream signal regulation modules into the iBN-uA-dSP, we added two new nodes to the network, which we termed Consume nodes (Fig. 5a). Consume 1N and Consume 2N produce the complements of rO_1 and rO_2, respectively, which consume their targets by hybridizing to them to create inert complexes (Fig. 5b). As RNA degradation is slower than RNA production, downregulating signal expression via the production of a complementary RNA should enable a faster downstream response. Biology has developed similar strategies to rapidly downregulate gene expression in cellular GRNs through antisense RNA hybridization[61]. Signal consumption through hybridization is similar to the mechanism used with the inducer RNAs to rapidly switch states in the iBN by consuming the repressors and it has also been successfully implemented in other genelet[21,43] and nucleic acid-based circuits[56]. To allow a single upstream input to simultaneously direct the network to switch states and to consume the current downstream signal, we programmed the Consume nodes to be activated by the same inputs as corresponding Induce nodes in a fan-out architecture (Fig. 5a). We termed this network the iBN with upstream activation and fan-out and downstream signal production and consumption (iBN-uAFO-dSPC).

The integrated induction and downstream signal regulation modules of the iBN-uAFO-dSPC resemble a coherent type-III feed-forward loop, in which an upstream node both directly represses a downstream node and activates a third node that also represses the downstream node[6,62]. In the iBN-uAFO-dSPC, activation of paired Consume and Induce nodes initiates both direct inactivation of the downstream signal via the Consume node and permanent repression of downstream signal production via the Induce node's activation of the Core node in the new state.

We sought to use the feed-forward design of the iBN-uAFO-dSPC to orchestrate a state change where the downstream signal of a given state is completely consumed before the network finishes changing states, enabling mutually exclusive expression of the downstream signals. This behaviour should be achieved if the Consume RNA production rate is higher than the corresponding downstream RNA production rate. To satisfy this condition, we included each Consume genelet at a threefold higher concentration than its corre-

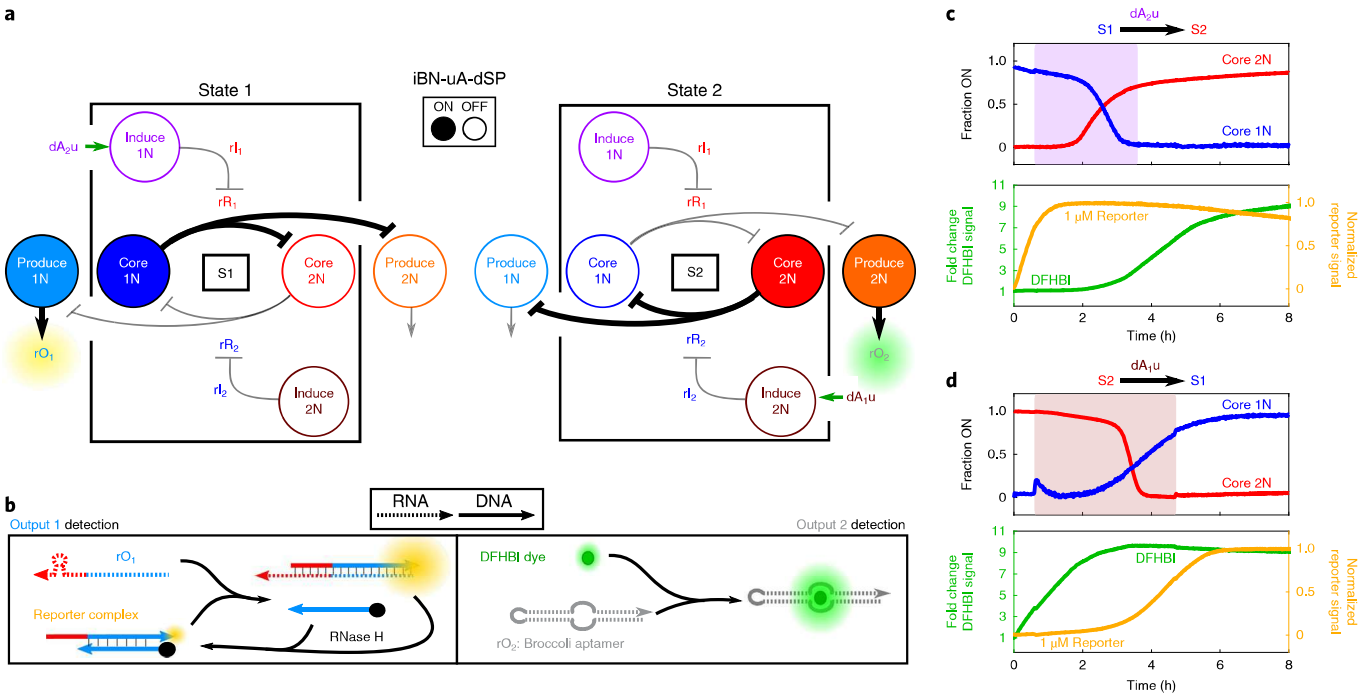

Fig. 4 | Connecting the iBN-uA to downstream nodes enables switching between the production of different downstream RNA signals. a, The architecture of the iBN-uA-dSP in each stable steady state. The iBN-uA (boxed) is connected to downstream Produce nodes that encode distinct RNA outputs. State changes are induced by activating the respective Induce nodes (indicated by the green arrows). **b**, The reactions used to detect the Produce nodes' RNA outputs ; rO_1 was detected via displacement of a quenching strand in a double-stranded DNA fluorophore-quencher reporter complex, whereas rO_2 (the Broccoli aptamer) was detected via binding of the 3,5-difluoro-4-hydroxybenzylidene imidazolinone (DFHBI) fluorescent dye[71]. **c**,**d**, Normalized activation levels of network nodes (top plots) and accumulation of reporting signals (bottom plots) during a switch from S1 to S2 (**c**) or from S2 to S1 (**d**). The shaded regions in the top plots indicate when the Induce nodes were ON during the experiments. Induce node activators and repressors were added to a final concentration of 1 μM and 1.5 μM, respectively, for both state changes.

sponding Produce genelet. Initializing the iBN-uAFO-dSPC in each state resulted in the initial production of the designed state-specific downstream signal. Following induction of a state change, the initial downstream signal was rapidly consumed and entirely removed by the time the network switched states and began producing the new state's downstream signal (Fig. 5c,d). The iBN-uAFO-dSPC is thus able to successfully coordinate the timing of both state changes and downstream signal expression in response to upstream signals.

Discussion

Here, we have systematically expanded the functionality of a genelet network by successively integrating multiple functional circuit modules. The iBN-uAFO-dSPC network we constructed is able to coordinate the temporal regulation of downstream signal expression during state changes, enabling it to orchestrate transitions between mutually exclusive downstream signal expression states in response to upstream environmental cues. This network could be reprogrammed to regulate the expression of different state-specific RNA outputs by changing the transcription sequences of the Produce and Consume nodes, and multiple different outputs could be controlled in each state by incorporating additional Produce/Consume nodes with unique transcription sequences. The ability to include the Produce/Consume nodes at different concentrations and/or relative ratios suggests that RNA output production rates and steady-state concentrations should be tunable over a broad range. These properties could allow these networks to control state transitions between diverse nucleic acid-responsive materials such as nanostructures[36,39,49], hydrogels[63,64] and nanoparticles[49,65]. Similarly, the networks could control a wide array of downstream chemistries if the network outputs were programmed to be RNA aptamers that regulate the activity or availability of small molecules or enzymes[50,66]. Network outputs could also be coupled to additional genelet modules that execute more complex signal expression programs, or to other nucleic acid-based technologies such as DNA strand-displacement circuits[67] or DNA-templated chemical synthesis reactions[68], enabling these networks to execute and switch between state-specific chemical programs or synthesis pathways.

Reliably integrating genelet modules to construct the iBN-uAFO-dSPC required identification and mitigation of undesired interactions between network components. The original genelet design contained long single-stranded activator and repressor domains that, as the number of these domains increased, had a high propensity for cross-talk (Supplementary Section 8.4). The HPC genelet design limited circuit cross-talk and enabled us to consistently integrate additional functional modules into the network. This design could now facilitate the reliable expansion of other genelet networks or enable the de novo construction of networks with numerous orthogonal nodes (Supplementary Section 8.6). We also found that regulating the availability of RNA signals using a mechanism similar to anti-sense RNA regulation in cellular GRNs enabled an effective means of regulation that was faster than RNase H degradation in our networks, as demonstrated in the induction and downstream signal regulation modules. As this means of regulation is not specific to an individual module, modules that rely on complementary RNA hybridization for regulation may be straightforward to integrate into other genelet networks to obtain desired regulatory dynamics. Together the design principles elucidated here could make it possible to construct synthetic GRNs powerful enough to coordinate multiple chemical processes and repeatedly respond to different input signals with specific chemical programs.

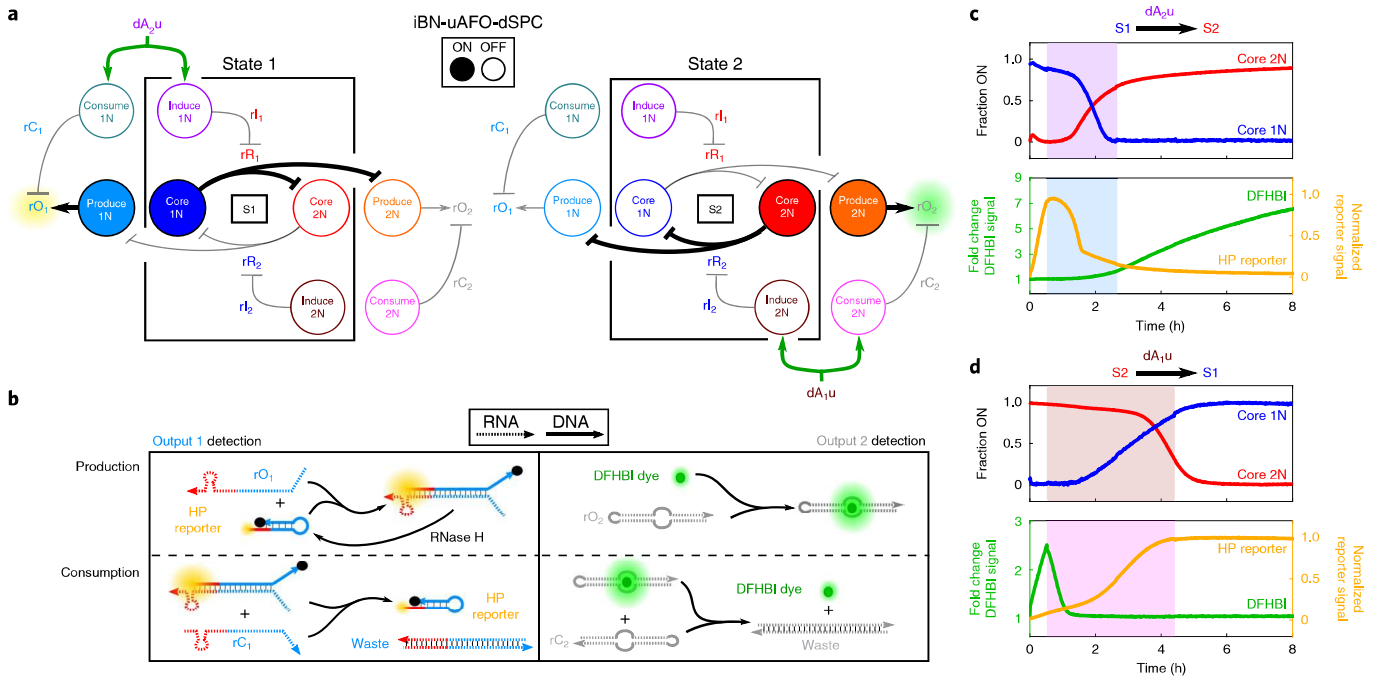

Fig. 5 | A fan-out feed-forward architecture enables mutually exclusive downstream signal expression states. a, The architecture of the iBN-uAFO-dSPC in each stable steady state. Paired Consume and Induce nodes are activated by the same input signal that initiates a state change (green arrows). **b**, The reactions used to detect production and consumption of the two downstream RNA outputs. A hairpin (HP) DNA reporter complex was used to detect rO_1, whereas rO_2 (the Broccoli aptamer) was detected via binding of the DFHBI fluorescent dye. Fluorescence increases or decreases as output concentration increases or decreases, respectively. The reporter complex for rO_1 was redesigned from Fig. 4b to minimize undesired interactions with rC_1. **c**,**d**, Normalized activation levels of network nodes (top plots) and RNA reporting signals (bottom plots) during a switch from S1 to S2 (**c**) or from S2 to S1 (**d**). The shaded regions in the plots indicate when the Induce nodes (top plots) and Consume nodes (bottom plots) were ON during the experiments. Activators and repressors used to initiate the state changes were added to final concentrations of 1 μM and 1.5 μM, respectively.

One challenge to developing these integrated synthetic regulatory networks is that in batch operation, inevitable fuel depletion and/or waste accumulation limits operational lifetime. We found that circuit lifetime decreased with network size: we could successfully switch the iBN and the iBN-uA twice but were unable to completely switch the iBN-uAFO-dSPC twice (Supplementary Fig. 37). Larger networks generally have higher transcriptional loads, which increases the rates of fuel depletion and waste accumulation (Supplementary Section 5.2). Thus, larger networks will probably require methods to manage fuel and waste products to allow them to operate long enough to perform their desired functions. For genelet circuits and other synthetic GRN analogues that require only a single fuel source and a few enzymes to be replenished in conjunction with global waste removal, the complexity of a waste and fuel management process may be independent of the network size.

Methods

Oligonucleotides, enzymes and other reagents. DNA and RNA sequences for all of the components are in Supplementary Table 1. All oligonucleotides were purchased from Integrated DNA Technologies, Inc. (IDT). Unmodified genelet DNA strands were purified by polyacrylamide gel electrophoresis by IDT. The DNA strands modified with fluorophores or quenchers were purified by high-performance liquid chromatography by IDT. The synthetic RNA repressor oligonucleotides were synthesized and purified under RNase-free conditions by high-performance liquid chromatography by IDT. Ribonucleotide triphosphates were purchased from ThermoFisher Scientific. The 3,5-difluoro-4-hydroxybenzylidene imidazolinone (DFHBI) fluorescent dye was purchased from Lucerna, Inc., prepared at 30 mM in dimethylsulfoxide and diluted to 1 mM in the New England Biolabs (NEB) RNAP reaction buffer for use in experiments; T7 RNAP was purchased in bulk (300,000 units) from Cellscript (270 U μl^{-1}, catalogue no. C-T7300K). Yeast inorganic pyrophosphatase was purchased from NEB (0.1 U μl^{-1}), RNase H was purchased from ThermoFisher Scientific (5 U μl^{-1}) and Bovine Serum Albumin was purchased from Sigma Aldrich (catalogue no. A3858). All genelets were annealed (90–20 °C cooling at 1 °C min^{-1}) in NEB RNAP reaction buffer with non-template and template strands at equimolar concentrations. The reporter complexes for the iBN-uA-dSP and blocked dA_2 were annealed under the same conditions with the strands of the complexes at equimolar concentrations. The hairpin reporter complex for the iBN-uAFO-dSPC (at 50 μM in NEB RNAP reaction buffer) was heated to 90 °C for 3 min and then immediately placed in ice water for 2 min before use in experiments.

Reaction conditions and data acquisition. Unless otherwise stated, network reactions were conducted at 37 °C in NEB RNAP reaction buffer supplemented with $MgCl_2$ (at a final concentration of 30 mM); ribonucleotide triphosphates (ATP, UTP, CTP, GTP, at a final concentration of 7.5 mM each); and Bovine Serum Albumin (at a final concentration of 0.1 mg ml^{-1}). In addition to T7 RNAP and RNase H, yeast inorganic pyrophosphatase was also included in the reactions (1.35×10^{-3} U μl^{-1}) to extend their transcriptional lifetime[69]. To avoid the need for the frequent recalibration that is required when using a new batch of T7 RNAP to account for batch-to-batch variation in enzyme activity[14,17,20,39,70], nearly all of the experiments in this study were conducted from a single bulk batch of T7 RNAP purchased from Cellscript. The bulk batch of T7 RNAP was split into smaller aliquots (enough for 20–30 experiments) to minimize the degradation of the enzyme resulting from repeated removal from the freezer. The concentrations of the DNA components and enzymes used for each network are tabulated in Supplementary Section 1.2. For the iBN-uA reactions, the Induce genelets were prepared with only 10% of the non-template strand modified with their respective fluorophores to avoid saturating the fluorescence signal. For the iBN-uA-dSP reactions, the rO_1 reporter complex was prepared with only 10% of the rO_1 reporter strand containing the TEX615 fluorophore to avoid saturating the fluorescence signal. All kinetic data were obtained in a quantitative PCR machine (Agilent Mx3000P) equipped with the standard filters: FAM/SYBR Green I (492–516 nm), HEX/JOE/VIC (535–555 nm), ROX/Texas Red (585–610 nm) and Cy5 (635–665 nm). A HEX filter was used to track TYE563, a Cy5 filter to track TYE665, a ROX fiilter to track TEX615 and a FAM filter to track FAM and the DFHBI–Broccoli aptamer signal. Fluorescence measurements were taken every minute during the reactions. The initial states of the networks were set by including the appropriate synthetic RNA repressor to a concentration in 10–50% excess of its corresponding activator before adding enzymes (rR_1s was added to set the network in S1 or rR_2s was added to set the network in S2). Before setting the initial state of

the network by adding the appropriate repressor, fluorescence measurements were taken while both Core nodes were in an ON state to obtain a minimum value for normalizing the activation levels. At the end of the experiments, DNA versions of both Core nodes' repressors were added in excess of their activators to obtain a reference for the maximum fluorescence value of each node. See Supplementary Section 12 for details on fluorescence data normalization procedures for all the different network experiments.

Data availability

The data that support the findings of this study are available from the corresponding authors on reasonable request.

Code availability

The MATLAB code that was used in the Supplementary Information to conduct the simulations presented in this study is available from the corresponding authors on reasonable request.

Received: 24 September 2018; Accepted: 13 June 2019;
Published online: 19 August 2019

References

1. Davidson, E. H. et al. A genomic regulatory network for development. *Science* **295**, 1669–1678 (2002).
2. Revilla-i-Domingo, R., Oliveri, P. & Davidson, E. H. A missing link in the sea urchin embryo gene regulatory network: *hesC* and the double-negative specification of micromeres. *Proc. Natl Acad. Sci. USA* **104**, 12383–12388 (2007).
3. Oppenheim, A. B., Kobiler, O., Stavans, J., Court, D. L. & Adhya, S. Switches in bacteriophage lambda development. *Annu. Rev. Genet.* **39**, 409–429 (2005).
4. Schultz, D., Wolynes, P. G., Jacob, E. B. & Onuchic, J. N. Deciding fate in adverse times: sporulation and competence in *Bacillus subtilis*. *Proc. Natl Acad. Sci. USA* **106**, 21027–21034 (2009).
5. Strmecki, L., Greene, D. M. & Pears, C. J. Developmental decisions in *Dictyostelium discoideum*. *Dev. Biol.* **284**, 25–36 (2005).
6. Alon, U. Network motifs: theory and experimental approaches. *Nat. Rev. Genet.* **8**, 450–461 (2007).
7. Peter, I. S. & Davidson, E. H. Assessing regulatory information in developmental gene regulatory networks. *Proc. Natl Acad. Sci. USA* **114**, 5862 (2017).
8. Tyson, J. J., Chen, K. C. & Novak, B. Sniffers, buzzers, toggles and blinkers: dynamics of regulatory and signaling pathways in the cell. *Curr. Opin. Cell Biol.* **15**, 221–231 (2003).
9. Weitz, M. et al. Diversity in the dynamical behaviour of a compartmentalized programmable biochemical oscillator. *Nat. Chem.* **6**, 295–302 (2014).
10. Ackermann, J., Wlotzka, B. & McCaskill, J. S. In vitro DNA-based predator–prey system with oscillatory kinetics. *Bull. Math. Biol.* **60**, 329–354 (1998).
11. Montagne, K., Plasson, R., Sakai, Y., Fujii, T. & Rondelez, Y. Programming an in vitro DNA oscillator using a molecular networking strategy. *Mol. Syst. Biol.* **7**, 466 (2011).
12. Semenov, S. N. et al. Rational design of functional and tunable oscillating enzymatic networks. *Nat. Chem.* **7**, 160–165 (2015).
13. Niederholtmeyer, H. et al. Rapid cell-free forward engineering of novel genetic ring oscillators. *eLife* **4**, e09771 (2015).
14. Kim, J. & Winfree, E. Synthetic in vitro transcriptional oscillators. *Mol. Syst. Biol.* **7**, 465 (2011).
15. Montagne, K., Gines, G., Fujii, T. & Rondelez, Y. Boosting functionality of synthetic DNA circuits with tailored deactivation. *Nat. Commun.* **7**, 13474 (2016).
16. Padirac, A., Fujii, T. & Rondelez, Y. Bottom-up construction of in vitro switchable memories. *Proc. Natl Acad. Sci. USA* **109**, E3212–E3220 (2012).
17. Subsoontorn, P., Kim, J. & Winfree, E. Ensemble bayesian analysis of bistability in a synthetic transcriptional switch. *ACS Synth. Biol.* **1**, 299–316 (2012).
18. Genot, A. J. et al. High-resolution mapping of bifurcations in nonlinear biochemical circuits. *Nat. Chem.* **8**, 760–767 (2016).
19. Postma, S. G. J., te Brinke, D., Vialshin, I. N., Wong, A. S. Y. & Huck, W. T. S. A trypsin-based bistable switch. *Tetrahedron* **73**, 4896–4900 (2017).
20. Kim, J., White, K. S. & Winfree, E. Construction of an in vitro bistable circuit from synthetic transcriptional switches. *Mol. Syst. Biol.* **2**, 68 (2006).
21. Kim, J., Khetarpal, I., Sen, S. & Murray, R. M. Synthetic circuit for exact adaptation and fold-change detection. *Nucleic Acids Res.* **42**, 6078–6089 (2014).
22. Helwig, B., van Sluijs, B., Pogodaev, A. A., Postma, S. G. J. & Huck, W. T. S. Bottom-up construction of an adaptive enzymatic reaction network. *Angew. Chem. Int. Ed.* **57**, 14065–14069 (2018).
23. Srinivas, N., Parkin, J., Seelig, G., Winfree, E. & Soloveichik, D. Enzyme-free nucleic acid dynamical systems. *Science* **358**, eaal2052 (2017).
24. Semenov, S. N. et al. Autocatalytic, bistable, oscillatory networks of biologically relevant organic reactions. *Nature* **537**, 656–660 (2016).
25. Kar, S. & Ellington, A. D. In vitro transcription networks based on hairpin promoter switches. *ACS Synth. Biol.* **7**, 1937–1945 (2018).
26. Kishi, J. Y., Schaus, T. E., Gopalkrishnan, N., Xuan, F. & Yin, P. Programmable autonomous synthesis of single-stranded. *DNA. Nat. Chem.* **10**, 155–164 (2017).
27. Orbán, M., Kurin-Csörgei, K. & Epstein, I. R. pH-Regulated chemical oscillators. *Acc. Chem. Res.* **48**, 593–601 (2015).
28. Whitesides, G. M. & Grzybowski, B. Self-assembly at all scales. *Science* **295**, 2418–2421 (2002).
29. Mattia, E. & Otto, S. Supramolecular systems chemistry. *Nat. Nanotechnol.* **10**, 111–119 (2015).
30. van Roekel, H. W. H. et al. Programmable chemical reaction networks: emulating regulatory functions in living cells using a bottom-up approach. *Chem. Soc. Rev.* **44**, 7465–7483 (2015).
31. van Esch, J. H., Klajn, R. & Otto, S. Chemical systems out of equilibrium. *Chem. Soc. Rev.* **46**, 5474–5475 (2017).
32. Whitesides, G. M. Reinventing chemistry. *Angew. Chem. Int. Ed.* **54**, 3196–3209 (2015).
33. Lehn, J.-M. Perspectives in chemistry—steps towards complex matter. *Angew. Chem. Int. Ed.* **52**, 2836–2850 (2013).
34. Garamella, J., Marshall, R., Rustad, M. & Noireaux, V. The all *E. coli* TX-TL toolbox 2.0: a platform for cell-free synthetic biology. *ACS Synth. Biol.* **5**, 344–355 (2016).
35. Zadorin, A. S. et al. Synthesis and materialization of a reaction–diffusion French flag pattern. *Nat. Chem.* **9**, 990–996 (2017).
36. Green, L. N. et al. Autonomous dynamic control of DNA nanostructure self-assembly. *Nat. Chem.* **11**, 510–520 (2019).
37. Postma, S. G. J., Vialshin, I. N., Gerritsen, C. Y., Bao, M. & Huck, W. T. S. Preprogramming complex hydrogel responses using enzymatic reaction networks. *Angew. Chem. Int. Ed.* **56**, 1794–1798 (2017).
38. Meijer, L. H. H. et al. Hierarchical control of enzymatic actuators using DNA-based switchable memories. *Nat. Commun.* **8**, 1117 (2017).
39. Franco, E. et al. Timing molecular motion and production with a synthetic transcriptional clock. *Proc. Natl Acad. Sci. USA* **108**, E784–E793 (2011).
40. Gines, G. et al. Microscopic agents programmed by DNA circuits. *Nat. Nanotechnol.* **12**, 351–359 (2017).
41. Karzbrun, E., Tayar, A. M., Noireaux, V. & Bar-Ziv, R. H. Programmable on-chip DNA compartments as artificial cells. *Science* **345**, 829–832 (2014).
42. Dupin, A. & Simmel, F. C. Signalling and differentiation in emulsion-based multi-compartmentalized in vitro gene circuits. *Nat. Chem.* **11**, 32–39 (2019).
43. Franco, E., Giordano, G., Forsberg, P.-O. & Murray, R. M. Negative autoregulation matches production and demand in synthetic transcriptional networks. *ACS Synth. Biol.* **3**, 589–599 (2014).
44. Kim, J., Hopfield, J. & Winfree, E. in *Advances in Neural Information Processing Systems* (eds Saul, L. K. et al.) 681–688 (MIT Press, 2005).
45. McAllister, W. T. in *Mechanisms of Transcription* Vol. 11 (eds Eckstein, F. & Lilley, D. M. J.) 15–25 (Springer Berlin, 1997).
46. Maslak, M. & Martin, C. T. Kinetic analysis of T7 RNA polymerase transcription initiation from promoters containing single-stranded regions. *Biochemistry* **32**, 4281–4285 (1993).
47. Osumi-Davis, P. A. et al. Bacteriophage T7 RNA polymerase and its active-site mutants: kinetic, spectroscopic and calorimetric characterization. *J. Mol. Biol.* **237**, 5–19 (1994).
48. Takinoue, M., Kiga, D., Shohda, K. & Suyama, A. Experiments and simulation models of a basic computation element of an autonomous molecular computing system. *Phys. Rev. E* **78**, 041921 (2008).
49. Jasinski, D., Haque, F., Binzel, D. W. & Guo, P. Advancement of the emerging field of RNA nanotechnology. *ACS Nano* **11**, 1142–1164 (2017).
50. Famulok, M., Hartig, J. S. & Mayer, G. Functional aptamers and aptazymes in biotechnology, diagnostics, and therapy. *Chem. Rev.* **107**, 3715–3743 (2007).
51. Milligan, J. F., Groebe, D. R., Witherell, G. W. & Uhlenbeck, O. C. Oligoribonucleotide synthesis using T7 RNA polymerase and synthetic DNA templates. *Nucleic Acids Res.* **15**, 8783–8798 (1987).
52. Arnold, S. et al. Kinetic modeling and simulation of in vitro transcription by phage T7 RNA polymerase. *Biotechnol. Bioeng.* **72**, 548–561 (2001).
53. Kern, J. A. & Davis, R. H. Application of solution equilibrium analysis to in vitro RNA transcription. *Biotechnol. Prog.* **13**, 747–756 (1997).
54. Niederholtmeyer, H., Stepanova, V. & Maerkl, S. J. Implementation of cell-free biological networks at steady state. *Proc. Natl Acad. Sci. USA* **110**, 15985 (2013).
55. Zadeh, J. N. et al. NUPACK: analysis and design of nucleic acid systems. *J. Comput. Chem.* **32**, 170–173 (2011).
56. Cherry, K. M. & Qian, L. Scaling up molecular pattern recognition with DNA-based winner-take-all neural networks. *Nature* **559**, 370–376 (2018).
57. Kotani, S. & Hughes, W. L. Multi-arm junctions for dynamic DNA nanotechnology. *J. Am. Chem. Soc.* **139**, 6363–6368 (2017).
58. Groves, B. et al. Computing in mammalian cells with nucleic acid strand exchange. *Nat. Nanotechnol.* **11**, 287–294 (2016).

59. Del Vecchio, D., Ninfa, A. J. & Sontag, E. D. Modular cell biology: retroactivity and insulation. *Mol. Syst. Biol.* **4**, 161 (2008).
60. Franco, E., Del Vecchio, D. & Murray, R. M. Design of insulating devices for in vitro synthetic circuits. In *Proc. 48th IEEE Conference on Decision and Control (CDC) Held Jointly with 2009 28th Chinese Control Conference* 4584–4589 (IEEE, 2009).
61. Pelechano, V. & Steinmetz, L. M. Gene regulation by antisense transcription. *Nat. Rev. Genet.* **14**, 880–893 (2013).
62. Mangan, S. & Alon, U. Structure and function of the feed-forward loop network motif. *Proc. Natl Acad. Sci. USA* **100**, 11980–11985 (2003).
63. Lin, D. C., Yurke, B. & Langrana, N. A. Inducing reversible stiffness changes in DNA-crosslinked gels. *J. Mater. Res.* **20**, 1456–1464 (2005).
64. Fern, J. & Schulman, R. Modular DNA strand-displacement controllers for directing material expansion. *Nat. Commun.* **9**, 3766 (2018).
65. Rogers, W. B., Shih, W. M. & Manoharan, V. N. Using DNA to program the self-assembly of colloidal nanoparticles and microparticles. *Nat. Rev. Mater.* **1**, 16008 (2016).
66. Pfeiffer, F. & Mayer, G. Selection and biosensor application of aptamers for small molecules. *Front. Chem.* **4**, 25 (2016).
67. Zhang, D. Y. & Seelig, G. Dynamic DNA nanotechnology using strand-displacement reactions. *Nat. Chem.* **3**, 103–113 (2011).
68. O'Reilly, R. K., Turberfield, A. J. & Wilks, T. R. The evolution of DNA-templated synthesis as a tool for materials discovery. *Acc. Chem. Res.* **50**, 2496–2509 (2017).
69. Cunningham, P. & Ofengand, J. Use of inorganic pyrophosphatase to improve the yield of in vitro transcription reactions catalyzed by T7 RNA polymerase. *BioTechniques* **9**, 713–714 (1990).
70. Schwarz-Schilling, M. et al. in *Cell Cycle Oscillators: Methods and Protocols* Vol. 1342 (eds. Coutts, A. S. & Weston, L.) 185–199 (Springer New York, 2016).
71. Filonov, G. S., Moon, J. D., Svensen, N. & Jaffrey, S. R. Broccoli: rapid selection of an RNA mimic of green fluorescent protein by fluorescence-based selection and directed evolution. *J. Am. Chem. Soc.* **136**, 16299–16308 (2014).

Acknowledgements

The authors would like to thank E. Franco, L. Green, H. Subramanian and C. C. Samaniego for their help with the initial genelet experiments, and J. Fern for insightful conversations. S.S. was supported by National Science Foundation Graduate Research Fellowship DGE-1746891. Materials, supplies and R.S. were supported by the Department of Energy BES DE-SC001 0426.

Author contributions

S.W.S. conceived and designed the study, designed and performed the experiments, analysed and interpreted the data, and wrote the manuscript. R.S. conceived and supervised the study, interpreted the data and wrote the manuscript.

Competing interests

The authors declare no competing interests.

Additional information

Supplementary information is available for this paper at https://doi.org/10.1038/s41557-019-0292-z.

Reprints and permissions information is available at www.nature.com/reprints.

Correspondence and requests for materials should be addressed to S.W.S. or R.S.

Publisher's note: Springer Nature remains neutral with regard to jurisdictional claims in published maps and institutional affiliations.